International Conference on Renewable Energies and Power Quality (ICREPQ'16)
Madrid (Spain), 4th to 6th May, 2016
Renewable Energy and Power Quality Journal (RE&PQJ)
ISSN 2172-038 X, No.14 May 2016

Prototype of a simplified polar heliostat suitable for integration in buildings

M. Torres Roldán, M. Varo-Martínez and R. López-Luque
Research Group on Physics for Renewable Energy and Resources
University of Cordoba,
Campus of Rabanales, 14014 Cordoba (Spain)
Phone/Fax number:+0034 957 212068, e-mail:fa1torom@uco.es, mvaro@uco.es, fa1lolur@uco.es

Abstract

The increasing improvement of energy sustainability entails a raise in the use of heliostats in small applications. These devices aim to use direct radiation as a source of natural lighting, and they are also used as components for concentration systems in thermal and photovoltaic applications. Most technological developments published about heliostats up to now refer to concentration tower thermosolar power plants. Furthermore, they are orientated towards heliostats of big dimensions with large distances between the reflector and the focus. It is different, however, for urban applications, where smaller heliostats and lower distances travelled by reflected rays are proposed, and, consequently, greater errors in solar tracking are allowed.

This paper describes a new simple heliostatic system suitable for small applications. The main feature of this system is the possibility of controlling several heliostats with a unique engine. It must be highlighted that the system proposed uses a simple logic and has an easy electronic controller implementation.

Key words

Heliostat, Building Integrated Heliostats, Concentration Systems, Natural daylighting

1. Introduction

Among the solar technologies for buildings that have received more attention in the last ten years, those that use sun-tracking and solar concentration should be highlighted. According to this, Chemisana [1] presents a systematized study of these technologies applied to photovoltaic production or Buildings Integrated Concentrating Photovoltaic (BICPV) systems. Even though references to thermal concentration integrated systems are few, their advantages are known in the fields of energy polygeneration and small distributed energy systems. Thereby, González-Pardo et al. [2] analyze the integrability of small concentration systems based on heliostat fields distributed on building facades. Finally, it should be highlighted that heliostats found in literature, as well as those proposed by commercial undertakings specialized in this field [3-8], require two engines for its correct orientation and its own electronic controller. Opposite to this, in this paper a prototype of a simplified polar heliostat with the advantage of having a unique engine is presented. It also allows associations of heliostats sharing the same engine and, as a consequence, the same movement controller.

2. Description of the device

Since, as hypothesis, direct sun's rays must emerge parallel to the Earth's axis after their reflection on the polar heliostat, being redirected by secondary mirrors when necessary, the polar heliostat is considered, in an equatorial system (Fig.1), as a mirror whose normal vector $\vec{\boldsymbol{n}}_{\boldsymbol{m}}$ is located in the bisectrix of the angle formed by $\vec{\boldsymbol{k}}$ (unitary vector in the direction of the OZ axis, that is, parallel to the Earth's rotation axis) and the sun vector, $\vec{\boldsymbol{s}}$ (Eq.1).

$$\vec{n}_m = \frac{\vec{s}+\vec{k}}{|\vec{s}+\vec{k}|} \qquad (1)$$

where, according to the fundamentals of Astronomy, the sun vector can be defined as a function of the declination (δ) and the angular velocity Ω by means of Eq. (2)

$$\vec{s} = \cos\delta \sin \Omega t\, \vec{i} + \cos\delta \cos \Omega t \vec{j} + \sin\delta\, \vec{k} \qquad (1)$$

Due to the fact that vectors $\vec{s}$and $\vec{k}$ form an angle of (π/2-δ), as it can be seen in Figure 1, the angle between $\vec{\boldsymbol{n}}_{\boldsymbol{m}}$ and $\vec{\boldsymbol{k}}$ - denoted as α - will be half the previous angle (Equation 3)

$$\alpha = \frac{\pi}{2} - \frac{\delta}{2} \qquad (3)$$

As a consequence, the movement of the normal vector to the mirror of a polar heliostat can be expressed by Equation 4.

$$\overrightarrow{n_m} = \cos\alpha \sin \Omega t\, \vec{i} + \cos\alpha \cos \Omega t \vec{j} + \sin\alpha\, \vec{k} \qquad (4)$$

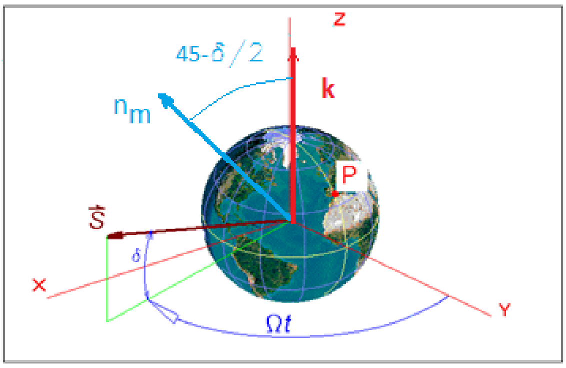

Fig. 1 Considered vectors for the proposed heliostat in an equatorial reference system.

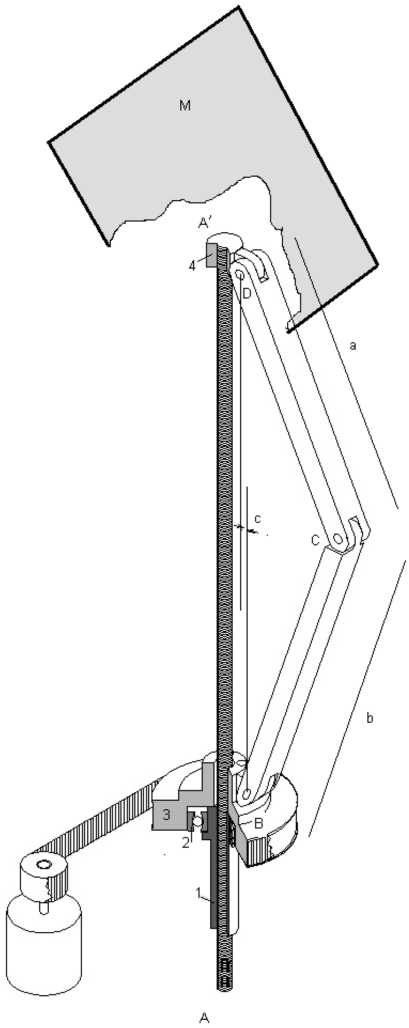

Fig. 2 Proposed polar heliostat in an equatorial reference system.

3. Mechanical principles of the proposed design

The presented heliostat consists of a simple mechanism and an electronic control system that allows the mirror normal vector to approach the movement described in Equation 4.

Figure 2 shows the scheme of the proposed mechanism. It has a rotation axis A-A' and a deformable quadrilateral with two bars of a fixed length, and it is articulated in points B, C and D. The first bar, CD, is a bar of a fixed length "a" that is articulated in points C and D. This bar is attached to support 4, soldered in the superior extreme of the axis A-A', connected through a hinge with one degree of freedom (1 dof) in point D. The second bar, BC, forms the deformable arm. It has a fixed length "b" and it is articulated in points C and B. As a result, both bars (CD and BC) are articulated between them in the common point C (1 dof). In the opposite extreme, bar BC is attached to piece 3 with a hinge (1 dof). The distance between the articulation B and the axis A-A', measured in the perpendicular direction to the axis, is fixed, and denoted as "c".

Piece 3 is a jagged wheel that rotates because of the action of a belt moved by an engine in the horizontal plane, remaining at a fixed height with respect to the horizontal plane in which the heliostatic device is installed. Wheel 3 directs the rotation of axis A-A', so that it moves vertically, screwing itself to screw 1. Besides, screw 1 is fixed to the Earth with a support and with the bearing 2, which allows the rotation of the wheel 3 with respect to the screw 1. Consequently, the rotation of the axis A-A' continues parallel to the Earth's rotation axis. Moreover, the three articulations in B, C and D will force bars BC and CD to remain in the same plane of axis A-A'.

Finally, mirror M is supported on the bar CD of the deformable arm. The plane of the mirror will be perpendicular to the plane that has the deformable polygon. This device will be fixed to the Earth, by checking that axis A-A' remains parallel to the Earth's axis. Moreover, it is advisable to check that the quadrilateral is contained in the meridian plane (vertical plane with direction N-S) at the moment of solar midday.
Regarding the described mechanism, the movement of the wheel 3 will cause that axis A-A' turns around the fixed screw 1. This leads to a change in the distance between points B and D and, consequently, in angle β between the axis A-A' and the bar CD, on which mirror M is supported.

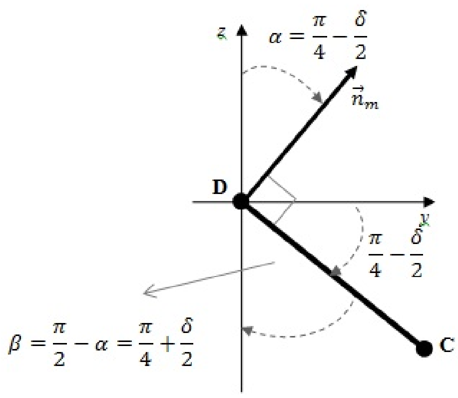

Fig. 3. Angles between the normal vector of the mirror and the Earth's rotation axis.

Figure 3 shows that, according to the geometry described and since the normal vector to the mirror will be always perpendicular to bar CD, angle β is equal to the complementary angle formed by the normal vector to the mirror and vector $\vec{k}$. As previously explained, for a perfect alignment of the mirror, the angle between the normal vector to the mirror and vector $\vec{k}$ will be given by Equation 4. Moreover, for an optimal alignment, angleβ will be given by Equation 5.

$$\beta = \frac{\pi}{2} - \alpha = \frac{\pi}{4} + \frac{\delta}{2}. \qquad (5)$$

According to this, and keeping in mind the annual variation interval of declination, $[-\delta_{max}, +\delta_{max}]$, it is essential to consider that the value of angle β may change in the interval $\left[\frac{\pi}{4} - \frac{\delta_{max}}{2}, \frac{\pi}{4} + \frac{\delta_{max}}{2}\right]$. This interval imposes restrictions in the design of the device.

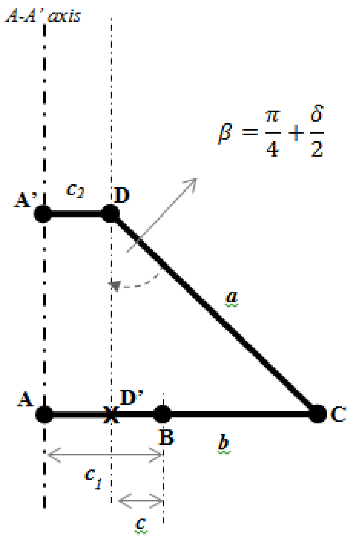

Fig. 4. Heliostat geometric restrictions.

This affects mainly to the dimension of the arms, due to the fact that some combinations do not allow that the real variation interval of angleβ has all the values required, even though the arm BCD is deformable. Figure 4 shows the extreme disposition that could be obtained with the maximum value of angleβ. Accordingly, the system geometry must always meet the restriction imposed by Equation 6.

$$c + b \geq a \cdot sen\left(\frac{\pi}{4} + \frac{\delta_{\max}}{2}\right) \qquad (6)$$

The mechanism described here is controlled only by the turn of the wheel 3, which performs two types of movement. The first necessary movement is due to the height variation of the sun trajectory, and aims to orientate the mirror according to it, while trying that angle β - formed by bar CD and axis A-A´ - approaches as much as possible to the angle given by Equation 5, as previously justified. This movement thus only depends on declination and, as a consequence, on the Julian day. This entails that it will only change once a day, preferably during the night hours. This movement will be determined by the whole number of turns "i" around the axis A-A' in the correct direction, which will change the distance from points B and D to axis A-A', and consequently angle β.

The objective of the second movement is to follow the sun throughout the day. It consists of a turn at a constant velocity and equal to Ω, and it begins with the sunrise and finishes at sunset. At that moment, the device returns in the inverse direction to wait for the sunrise of the following day. The daily movement makes that the plane defined by the sun vector, and the OZ axis coincides with the plane that contains the deformable polygon.

The position of the device at each moment, thereby, will be given by the superposition of the two movements previously described. The algorithm for the calculation of the magnitudes associated to both movements has been described in detail a previous paper [9].

In that way, thanks to the mechanism described in this paper, rays will be reflected in a direction near the screw axis or the Earth's rotation axis. It is unavoidable, however, the existence of a systematic error due to the geometry of the different components. This systematic error, as studied in the following part of this paper, mainly depends on the screw thread pitch, p.

Finally, it is important to highlight that the device allows the association of different heliostats, so that they can be moved by a unique engine (Figure 5). Moreover, it also allows its application to solar concentration systems with the disposition of secondary mirrors.

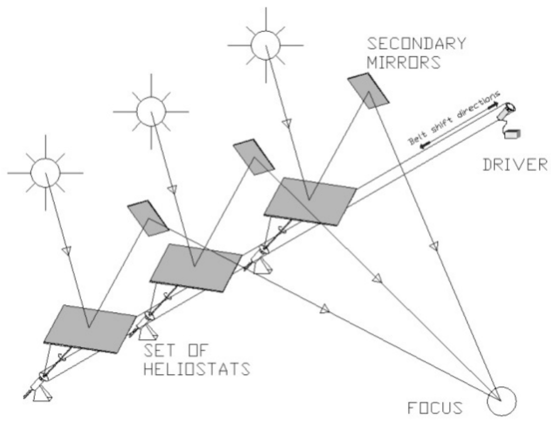

Fig. 5. Proposal of association of several devices to be moved with a unique engine and of the use of secondary mirrors.

4. Description of an experimental prototype of the device proposed

In order to actually assess the performance of the heliostat proposed, the experimental prototype shown in Figure 6and whose main features are presented in Table1 has been built.

The microcontroller Arduino Uno Rev.3 [10], a real-time clock module, and a step-by-step engine driver have been used to control the movements of the device, as previously described. Arduino Uno Rev.3 is a low-cost microcontroller (its price is less than $30 per unit) programmable in C language. The program-memory capacity of this microcontroller allows the real-time implementation and the calculation of the sun's position (Equations 1-5). It also determines the best approximation to equation 5 in real time, calculating for each day the optimal number of turns of axis A-A'. With this microcontroller, and thanks to a step-by-step engine (1200 steps per turn), it is possible to control the position of the heliostat.

Table 1. Main dimensions of the built prototype

Dimensions	
a=	300 mm
b=	324 mm
c=	20 mm
d_0 =	400 mm
p =	2 mm
Site: Córdoba (Spain)	
Latitude=	37,85 ºN
Longitude=	4,18 ºW

Fig. 6.Photograph of the prototype built

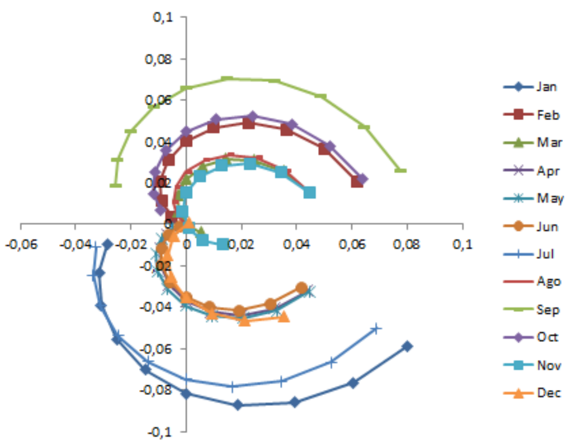

Fig. 7. Trajectories of incidence point for the 15th of each month respect the target point. Coordinates are given in m.

To characterize the pointing errors due to the geometry of the device, a focal point located 12,66 m from the main mirror was considered as a target. Figure 7 shows, for the 15th of each month, the trajectories of the incident rays at different hours and their deviation from the target point, whose coordinates are (0,0) m. In terms of angular errors, it is found that the average pointing error of the device is $\bar{\varepsilon}$=2.96 mrad, with a standard deviation of σ_{ε}=3.11 mrad.

5. Conclusions

This paper presents a mechanism for a polar heliostatic device composed of an arm deformable due to the rotary movement of an axis A-A' parallel to the Earth's axis (Figure 1). The innovation of this device is that it only needs an action for its positioning, both in elevation and in azimuth. Moreover, it also allows the association of different heliostats, so that they can be moved by a unique engine. This also enables the use of the device for solar concentration techniques thanks to the disposition of secondary mirrors.

The mechanism proposed is really simple, so a very competitive price is expected for a quantity production. The simplicity of the mechanism, however, leads to the existence of some systematic errors since the movement of the mirror of the heliostat around its axis A-A', is not continuous, but in discrete jumps depending on the thread pitch of the axis. The study of errors carried out shows the possibility of obtaining average acceptable errors, especially in urban applications

6. References

[1] Chemisana, D. Building integrated concentrating photovoltaics: a review. Renewable and Sustainable Energy Reviews, 15.1 (2011), 603-611.
[2] Gonzalez-Pardo, A., Cesar Chapa, S., Gonzalez-Aguilara, J., & Romero, M. Optical performance of vertical heliostat fields integrated in building facades for concentrating solar energy uses. Solar Energy, 97 (2013), 447–459.
[3] Heliostat (http://www.heliostaat.nl/index.html). Retrieved in October 2015.
[4] Practical Solar (http://www.practicalsolar.com/index.html). Retrieved in October 2015.
[5] Solar Mems Technologies (http://www.solar-mems.com/es/). Retrieved in October 2015.
[6] Lumena (http://www.lumena.ch/index.htm) Retrieved in October 2015.
[7] Carpenter Norris Consulting (http://www.carpenternorris.com/). Retrieved in October 2015
[8] Egis Offenbanch (http://egis.org/helio_us.html). Retrieved in October 2015.
[9]Torres-Roldán M., López-Luque R., Varo-Martínez M.Design of an innovative and simplified polar heliostat for integration in buildings and urban environments.Solar Energy, 119 (2015), 159–168.
[10] Arduino Website (http://arduino.cc/en/Main/arduinoBoardUno). Retrieved in October 2015.